An Application of the Impedance Boundary Condition to Microwave Cavity Analysis using Vector Finite Element Method

Pan-Seok Shin*, Changyul Cheon and Sheppard J. Salon*****

Abstract - This paper presents an application of an impedance boundary condition to 3D vector finite element analysis of a multi-port cylidrical microwave cavity using Snell's law. Computing memory benefits and computing time reduction are obtained from this method compared with the conventional finite element method(FEM). To verify the method, a high permittivity scatterer in free space is analyzed and compared with the results of conventional (FEM). In addition, this method has been analyzed several types of cavities, including water load, to demonstrate the validity and accuracy of the program.

Keywords: microwave cavity, vector finite element method, edge element, impedance boundary condition.

1. Introduction

The conventional impedance boundary condition (IBC) has become extensively applied to radio frequency devices and various electromagnetic problems, such as eddy current, induction heating, and scattering[1-3]. The IBC states that the ratio of the tangential component of the surface electric field to the tangential magnetic field at the surface of a part experiencing eddy current is a constant ratio, and this constant is called the surface impedance. The IBC is an approximate boundary condition that is applicable at the surface of materials experiencing pronounced skin effect. The use of the IBC allows the elimination of bodies made of such materials from the field solution region at great savings in computing cost. However, the IBC is an approximation that is applicable only under certain limited conditions and is justified from Maxwell's equation. Since the IBC has become very important through its wide application, S. R. Hoole [1] has validated the IBC using a laboratory experiment and reviewed the limitations of the IBC so that its proper use may be established.

N. Ida and S. Yuferev [4] have derived the approximate boundary conditions for the tangential components of the electric field and the normal component of the magnetic field on the surface of a homogeneous body of finite conductivity (conductor or lossy dielectric) for the transient incident electromagnetic field. They have also introduced scale factors for basic variables in such a way that a small parameter, proportional to the ratio of the penetration depth and body's characteristic size, appears in the dimensionless Maxwell's equations for the conducting region. They then used the perturbation method.

S. M. Mimoune and his group [5] have presented a study of 3D magneto-thermal finite element phenomena. The (A,V-A) formulation using the IBC was applied to multiply connected regions. From the exterior inductor voltage and current density distribution, the impedance and the total power of the induction heating devices are calculated. B. Dumont and A. Gannoud [6] proposed an iterative method to model an electromagnetic shaping of molten metal by using the IBC with moving FEM mesh to improve the high frequency configuration.

We present an IBC using Snell's law (SIBC) to analyze a multi-source microwave cavity. A finite element analysis of a 3D microwave cavity including high dielectric load such as water load or high water content load has suffered from long computing time and large computer memory size since the high dielectric constant require a huge number of meshes. These difficulties are overcome by using a Vector Finite Element Method (VFEM), which uses edge elements and the SIBC. The wave equation is formulated by Galerkin's weighted residual FEM using 3D tetrahedral edge element [7]. In addition, the parallelized QMR method [8] is employed to solve the system matrix of the proposed models. In the paper, several example models including a scatterer and a cylindrical cavity are provided to verify the formulation of the FEM program. Also, a two-port rectangular cavity model is designed, manufactured, and tested to compare with the calculated and measured results.

* Electrical Engineering Department of Hongik University, Jochiwon, Chungnam, 339-701, Korea (e-mail: psshin@hongik.ac.kr).
** University of Seoul, Seoul Korea(e-mail: changyul@uoscc.uos.ac.kr).
*** Rensselaer Polytechnic Institute, Troy, New York 12180, USA (e-mail: salons@rpi.edu).
Received October 2, 2002 ; Accepted December 26, 2002

2. Numerical Formulation

2.1 Three-Dimensional FEM for Wave Equation

A vector wave equation for the electric field, E, is derived from the Maxwell Equation:

$$\nabla\times(\mu_r\times E)-k_0^2\varepsilon_r\vec{E}=0 \tag{1}$$

$$\hat{n}\times\vec{E}=0 \tag{2}$$

where k_0 is the propagation constant ($k_0=\omega\sqrt{\varepsilon_0\mu_0}$), ω is angular frequency, μ_r is a relative permeability, ε_r is a dielectric constant, and all the walls of the cavity are assumed to be perfect conductors. The boundary conditions often encountered are those to be applied at electrically conducted surfaces as in Eq. (2).

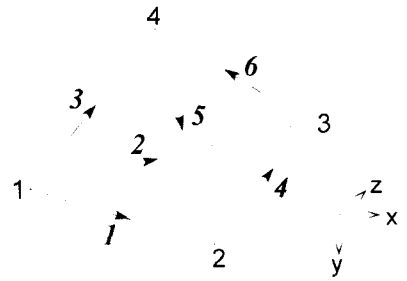

Fig. 1 A tetrahedral edge element for FE formulation

Fig. 1 shows a tetrahedral edge element to discretize the microwave cavity and waveguide. A vector basis function can be derived using the 3D interpolation function, L_i:

$$L_i=\frac{a_i+b_ix+c_iy+d_iz}{6V} \tag{3}$$

where a_i, b_i, c_i, and d_i are coefficients determined by the coordinate of the related nodes, subscript i is the node number (1,2,3,4), and V is the volume of the element.

$$a_i=\begin{vmatrix}x_{i+1} & x_{i+2} & x_{i+3}\\ y_{i+1} & y_{i+2} & y_{i+3}\\ z_{i+1} & z_{i+2} & z_{i+3}\end{vmatrix} \tag{4}$$

$$b_i=\begin{vmatrix}1 & 1 & 1\\ y_{i+1} & y_{i+2} & y_{i+3}\\ z_{i+1} & z_{i+2} & z_{i+3}\end{vmatrix} \tag{5}$$

$$c_i=\begin{vmatrix}1 & 1 & 1\\ x_{i+1} & x_{i+2} & x_{i+3}\\ y_{i+1} & y_{i+2} & y_{i+3}\end{vmatrix} \tag{6}$$

$$d_i=\begin{vmatrix}1 & 1 & 1\\ y_{i+1} & y_{i+2} & y_{i+3}\\ x_{i+1} & x_{i+2} & x_{i+3}\end{vmatrix} \tag{7}$$

Using L_i, the vector basis function, N_i, can be formulated as

$$\vec{N}_i=L_{i1}\nabla L_{i2}-L_{i2}\nabla L_{i1} \tag{8}$$

where i is the number of the edge element and where $i1$ is the starting node and $i2$ the ending node number of the i-th edge. In the element, the electric field vector, E, is

$$\vec{E}=\sum_{i=1}^{6}\vec{N}_iE_i, \tag{9}$$

where $Ei=\int_l\vec{E}\cdot d\vec{l}_i$.

The FEM formulation of the vector wave equation (Eq.(1)) is performed by using Galerkin's Weighted Residual method as follows:

$$\int_\Omega\vec{N}_i\cdot\left(\nabla\times\left(\frac{1}{\mu_r}\nabla\times\vec{E}\right)-k_0^2\varepsilon_r\vec{E}\right)d\Omega=0 \tag{10}$$

where $\vec{N}_i$ is used as a weighting function and Ω is the 3D problem domain. Using the vector identity and integral operation, Eq.(10) can be modified as,

$$\int_\Omega\left[\frac{1}{\mu_r}(\nabla\times\vec{N}_i)\cdot(\nabla\times\vec{E})-k_0^2\varepsilon_r\vec{N}_i\cdot\vec{E}\right]d\Omega+\int_\Gamma\vec{N}_i\cdot(\hat{n}\times\frac{\nabla\times\vec{E}}{\mu_r})d\Gamma=0 \tag{11}$$

where $\hat{n}$ is the outward normal unit vector of boundary and Γ is the surface boundary. The boundary integration over the conducting wall becomes zero by choosing the appropriate basis function. When considering scatterer in free space, the boundary integral is treated using the conventional absorbing boundary condition (ABC). An electric field on the boundary surface of the port is expressed, with the assumption that only TE*mo* modes exist, as

$$\begin{aligned}\vec{E}(x,y,z) &= \vec{E}^{inc} + \vec{E}^{ref} \\ &= \hat{y}E_0 \sin(\frac{\pi x}{a})e^{-jkz} + \hat{y}RE_0 \sin(\frac{\pi x}{a})e^{jkz}\end{aligned} \tag{12}$$

where E_0 denotes the magnitude of the incident wave and R denotes the reflection coefficient. The boundary integral in Eq.(11) can be treated using the following equation.

$$\begin{aligned}&\hat{n}\times(\hat{n}\times\vec{E}) = -\vec{E}, \\ &\hat{n}\times\nabla\times\vec{E} = -jk\vec{E}^{inc} + jk\vec{E}^{ref} \\ &= jkE - 2jk\vec{E}^{inc} = -\gamma\hat{n}\times(\hat{n}\times E) + \vec{U}^{inc}\end{aligned} \tag{13}$$

where $\gamma = jk$, $\vec{U}^{inc} = -2jk\vec{E}^{inc}$.

Using Eq.(13) and a vector identity, the surface integral of Eq.(11) can be rewritten as

$$\begin{aligned}&\int_\Gamma \vec{N}_i \cdot (\hat{n}\times\frac{\nabla\times\vec{E}}{\mu_r})d\Gamma \\ &= \int_\Gamma \frac{1}{\mu_r}\left[\gamma(\hat{n}\times\vec{N}_i)(\hat{n}\times\vec{E}) + \vec{N}_i\cdot\vec{U}^{inc}\right]d\Gamma.\end{aligned} \tag{14}$$

The first term of Eq.(11) can be discretized using Eq.(9) and Eq.(10). Thus, the coefficient matrix equation is

$$[[K]+[M]+[B]]\{E\} = \{F\} \tag{15}$$

where the elements of the coefficient matrix are

$$k_{ij} = \int_{\Omega e}(\frac{1}{\mu_r^e})(\nabla\times N_i^e)(\nabla\times N_j^e)d\Omega \tag{16}$$

$$m_{ij} = \int_{\Omega e} k_0^{\,2}\varepsilon_r^{\,e} N_i^e \cdot N_j^e \, d\Omega \tag{17}$$

$$b_{ij} = \int_{\Gamma^e}(\frac{r}{\mu_r^e})(\hat{n}\times N_i^e)(\hat{n}\times N_j^e)d\Gamma \tag{18}$$

$$\begin{aligned}f_i &= \int_{\Gamma^e}(\frac{1}{\mu_r^e})N_i^e \cdot U^{e\ inc}\, d\Gamma \\ &= \frac{jkA^e}{9\mu_r^e}\cdot\sin\left(\frac{x_c^e - x_b}{x_a}\pi\right)\cdot(c_{i1} - c_{i2}).\end{aligned} \tag{19}$$

Using the vector identities, k_{ij} , m_{ij}, and b_{ij} can be calculated as functions of the coefficients of the interpolation function, L_i.

$$\begin{aligned}k_{ij} = \frac{1}{324\ \mu_r^e}&\left[(c_{i1}^e d_{i2}^e - d_{i1}^e c_{i2}^e)(c_{j1}^e d_{j2}^e - d_{j1}^e c_{j2}^e)\right. \\ &+ (d_{i1}^e b_{i2}^e - b_{i1}^e d_{i2}^e)(d_{j1}^e b_{j2}^e - b_{j1}^e d_{j2}^e) \\ &\left.+ (b_{i1}^e c_{i2}^e - c_{i1}^e b_{i2}^e)(b_{j1}^e c_{j2}^e - c_{j1}^e b_{j2}^e)\right]\end{aligned} \tag{20}$$

$$\begin{aligned}m_{ij} = k_0^{\,2}\varepsilon_{r2}&\left[coef\ (i1,j1)(b_{i2}^e b_{i2}^e + c_{i2}^e c_{i2}^e + d_{i2}^e d_{i2}^e)\right. \\ &+ coef\ (i2,j2)(b_{i1}^e b_{i1}^e + c_{i1}^e c_{i1}^e + d_{i1}^e d_{i1}^e) \\ &- coef\ (i1,j2)(b_{i2}^e b_{i1}^e + c_{i2}^e c_{i1}^e + d_{i2}^e d_{i1}^e) \\ &\left.- coef\ (i2,j1)(b_{i1}^e b_{i2}^e + c_{i1}^e c_{i2}^e + d_{i1}^e d_{i2}^e)\right]\end{aligned} \tag{21}$$

$$\text{where } coef(i,j) = \begin{cases}1/720V^e, & i \neq j \\ 1/320V^e, & i = j.\end{cases} \tag{22}$$

$$\begin{aligned}b_{ij} = \frac{\gamma}{\mu^{r\,e}}&\left[coef\ (i1,j1)(c_{i2}^e c_{i2}^e + b_{i2}^e b_{i2}^e)\right. \\ &+ coef\ (i2,j2)(c_{i1}^e c_{i1}^e + b_{i1}^e b_{i1}^e) \\ &- coef\ (i1,j2)(+ c_{i2}^e c_{i1}^e + d_{i2}^e d_{i1}^e) \\ &\left.- coef\ (i1,j2)(c_{i1}^e c_{i2}^e + b_{i1}^e b_{i2}^e)\right]\end{aligned} \tag{23}$$

$$\text{where } coef(i,j) = \begin{cases}A^e/432(V^e)^2, & i \neq j \\ A^e/216(V^e)^2, & i = j.\end{cases} \tag{24}$$

2.2 Impedance Boundary Condition

When a microwave cavity is analyzed by the FEM, at least ten elements are required on a wavelength. Especially in high permittivity or high permeability materials, a huge number of elements is required to solve the field problem properly because the wavelength becomes very short. These kinds of problems can be solved using the IBC.

The basic concept of the IBC [1] is that an electric and magnetic field parallel to a boundary is unaffected by the other EM field and is determined by only its own material properity on the boundary. The SIBC method is applied under the assumptions that the skin depth of the material is small, the boundary is smooth, and the incident wave right inside the high dielectric medium is normal to the boundary plane by Snell's law. These assumptions can be properly applied to the water load or the high water contents load. In the modified impedance boundary condition (MIBC) an incident angle of the wave and its curvature of the boundary are considered to calculate the field.

On the boundary, the electric and magnetic field parallel to the boundary is continuous and the ratio of the electric

field to the magnetic field in air bounded by a high permittivity material (e.g. a water load) is the same as the intrinsic impedance of the load. The relationship can be expressed by

$$\hat{n} \times \vec{E} = -Z_s \cdot \hat{n} \times \left(\hat{n} \times \vec{H}\right) \tag{25}$$

$$\hat{n} \times n \times \vec{E} = Z_s \cdot \hat{n} \times \nabla \times \frac{1}{j\omega\mu} \hat{E} \tag{26}$$

where $\hat{n}$ is the unit vector toward the water load and Z_s is the impedance of the water load. Using Eqs.(25) and (26), the boundary integral term of Eq.(11) can be rewritten as

$$\int_\Gamma \vec{N}_i \cdot (\hat{n} \times \frac{\nabla \times \vec{E}}{\mu_r})\, d\Gamma = \int_\Gamma \vec{N}_i \cdot \left[\frac{j\omega\mu}{Z_s} \left(\hat{n} \times \vec{N}\right) \cdot \left(\hat{n} \times \vec{E}\right) \right] d\Gamma. \tag{27}$$

3. Examples of Applications

3.1 Verification of 3D FEM Program

For verifying the 3D FEM formulation of Eq.(11), a one-port cavity is analyzed as shown in Fig. 2. The cavity size is $405 \times 450 \times 55$ mm^3 with a port, whose width is 109 mm. TE_{10} mode (f = 2.45 GHz) is imposed on the boundary surface of the waveguide port, and its electric field distribution is calculated as shown in Fig. 2. The electric field is well distributed as expected.

In addition, a two-port microwave cavity (rectangular type) is designed and manufactured as a test model to verify the 3D FE program. The final model is determined after calculating the power dissipation as a function of the port position. There are three variables; x, y, and the cavity width as shown in Fig. 3(a). The maximum point of power dissipation occurs at x = 0 and y = 13.1 mm. Also, the minimum reflection and the maximum power dissipation occurs at a width of 35.5 mm. The final dimension of the model is fixed as $390 \times 360 \times 55$ mm^3 and the load size is $210 \times 210 \times 55$ mm^3. Fig. 3(b) shows an electric field ($|E|^2$) pattern of the model TE_{10} mode (f = 2.45 GHz) is imposed on the boundary surface of the wave guide port and its $|E|^2$ is calculated.

The scattering parameters are also calculated by using the two-port network method to compare with the measured values. For example, S_{11} can be derived from the product of H and the incident plane:

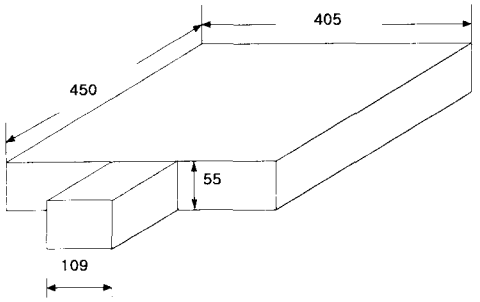

(a) One-port microwave cavity model($405 \times 450 \times 55$ mm^3)

(b) Electric field distribution of the cavity at z = 27.5 mm

Fig. 2 One-port microwave cavity model to verify the 3D edge element FE formulation

$$\vec{H} \cdot \hat{x} = \frac{-k\,\vec{E}^{inc}}{\omega\mu} \sin\frac{\pi x}{a} \left(e^{-jkz} - Re^{jkz}\right). \tag{28}$$

The R (= S_{11}) can be calculated by using Eq.(21) to put zero into z because the incident plane is the reference of the two-port network. The calculated parameters are compared with the measured data as shown in Table 1, which is a fairly good agreement within the tolerance of 5%.

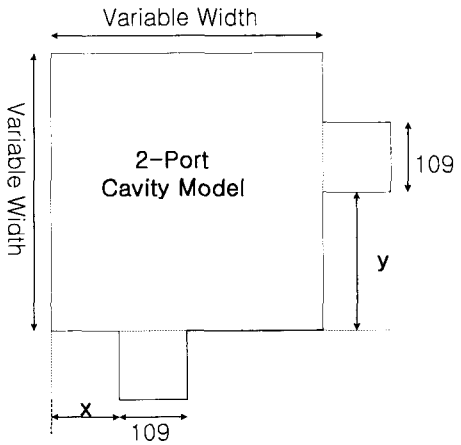

(a) Initial Model of the two-port cavity

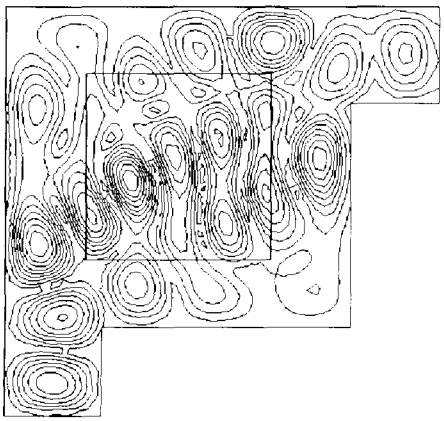

(b) Electric field distribution

Fig. 3 Electric field ($|E|^2$) contour lines of two-port Microwave cavity model (cavity size = 390×360 mm^2, load size = 210×210 mm^2)

Table 1 Comparison of S-parameters for the 2-port cavity model

S-parameters		Calculated	Measured
S_{11}	amplitude	0.9121	0.9051
	phase	59.85	62.83
S_{21}	amplitude	0.4981	0.5145
	phase	96.24	99.10
S_{22}	amplitude	0.8921	0.8762
	phase	-32.52	-34.69
S_{12}	amplitude	0.5020	0.5019
	phase	96.28	98.23

3.2 Examples of IBC Applications

A cylindrical microwave cavity with a waveguide is designed and simulated for verifying the proposed program with the IBC. The simulation results of the model are compared with the results of the conventional FEM without SIBC. As shown in Fig. 4(a), the radius of the cavity model is 258 mm and the radius of the water load ($\varepsilon_r = 80$) is 100 mm. The width of the waveguide is 86.36 mm and the length is 283.5 mm.

As shown in the figures, the two results are almost the same. It means that the incident angle cannot affect the impedance on the boundary. The number of edge elements is 13489 and the number of nodes is 4596 for the SIBC case. As shown in Table 2, computing memory size and computing time for the microwave cavity are reduced by nearly one half compared with the conventional method. TE_{10} mode (f = 2.45 GHz) is imposed on the boundary surface of the waveguide port and its E field distribution is analyzed as shown in Figs. 4(b) and 4(c). The dissipated power, P_{dis}, of the cavity is calculated using Eq.(29) and described in Table 2.

$$P_{dis} = \frac{1}{2}\mathrm{Re}\int_{\Gamma}(\vec{E}\times\vec{H}^{T})\cdot n\,d\Gamma = \frac{1}{2}\mathrm{Re}\int_{\Gamma}\frac{-j}{\omega\varepsilon}\,j\gamma\,(\hat{n}\times\vec{H})\cdot(\hat{n}\times\vec{H}^{T})\,d\Gamma \tag{29}$$

Table 2 Comparison of Computing Memory and Time for the Cavity Model

Variables	Conventional FEM	SIBC Method
No. of Nodes	9,742	4,596
No. of Elements	17,567	8,893
No. of Edges	26,455	13,489
CPU Time	1783 s	726 s
Incident Power	$1.7e^{-5}$ W	$1.8e^{-5}$ W

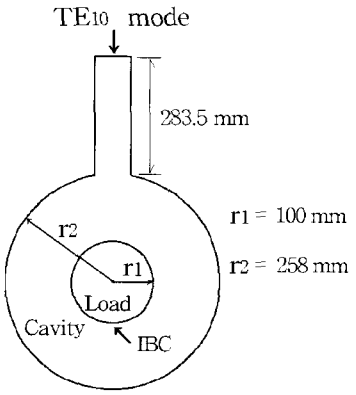

(a) Cylindrical MW cavity model

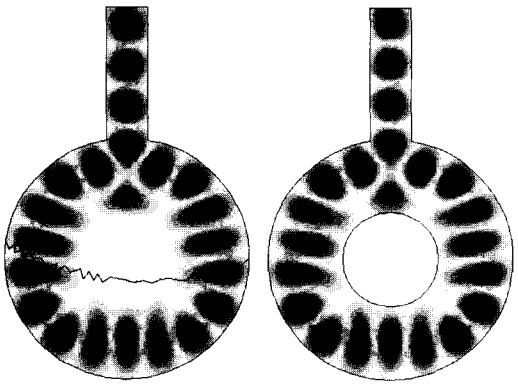

(b) Without SIBC (c) With SIBC

Fig. 4 Electric field distributions for cylindrical MW cavity and waveguide model

3.3 Three-Port Cylindrical Microwave Cavity

A three-port cylindrical microwave cavity, e.g., a clothes dryer, is simulated to analyze its electromagnetic field using the FEM program with SIBC. Fig. 5 shows the 3D model of the three-port cylindrical cavity. The radius of the cavity is 516 mm and its length is 372 mm. The distance between the two feeding ports is 93 mm, which is determined by the results of the power dissipation calculation for the simulation model. Fig. 6 shows the 3D tetrahedral

meshes of the model. The number of nodes and edges are 39,249 and 245,779 for the whole model with the proposed 3D FEM. The system matrix is solved by the parallelized QMR method by using HPC160, and the computing time is about 59 hours. Fig. 7(a) shows the E-field distribution of the model at $X = 80$ mm in the YZ plane, which is solved by the conventional 3D FEM without SIBC and Fig. 7 (b) shows the electric field distribution of the model at $Y = 0$ mm in the ZX plane. Fig. 7(c) shows the electric-field distribution of the model at $Z = 80$ mm in the XY plane without SIBC.

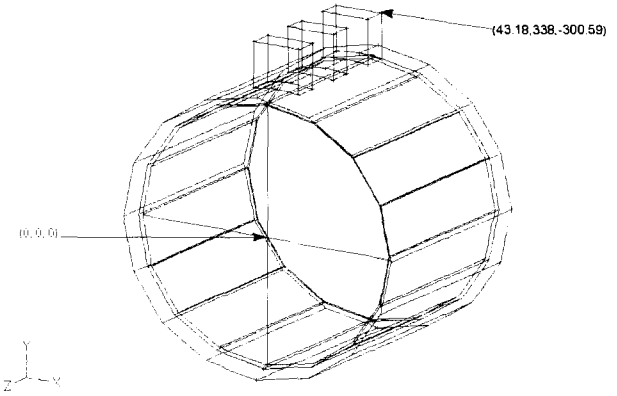

Fig. 5 3D simulation model of the three-port cylindrical cavity clothes dryer

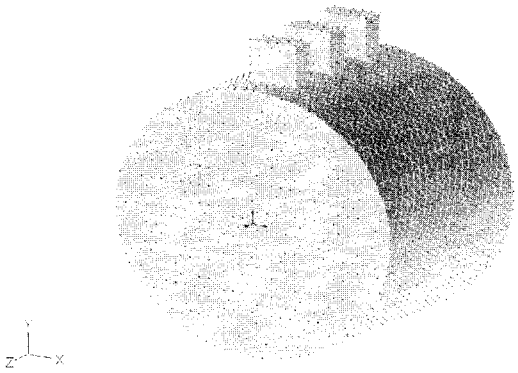

Fig. 6 Power dissipation of the test model as a function of port distance

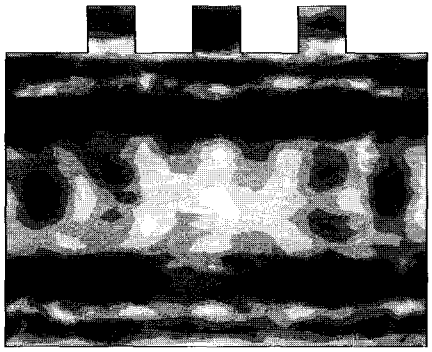

(a) Electric field in ZY plane at $X = 80$ mm (without SIBC)

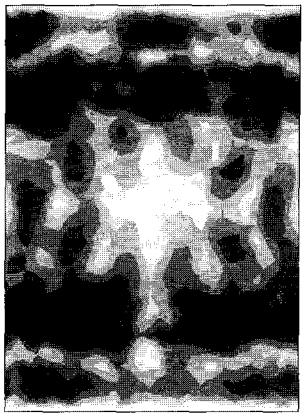

(b) Electric field in ZX plane at $Y = 0$ mm (without SIBC)

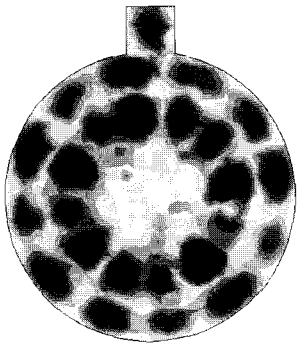

(c) Electric field in XY plane at $Z = 80$ mm

Fig. 7 Electric field distribution of the three-port microwave clothes dryer simulation model

On the other hand, the numbers of meshes for the SIBC case are dependent upon the size of the applied impedance boundary. When a cylindrical water load is inserted in the center of the cavity and the SIBC is applied on the boundary, the number of edges is reduced to 197,862. Also the computing time is reduced by about 18%.

4. Conclusion

This paper proposes an application of an IBC to a 3D vector finite element analysis of a multi-port microwave cavity using Snell's law. The wave equation is formulated using a tetrahedral edge element, and the IBC with Snell's law (SIBC) is imposed on the high permittivity material. For verifying the program, a scatterer and one and two-port microwave cavities are analyzed by the method as case studies. In addition, a three-port cylindrical microwave cavity is designed and analyzed by the proposed program. The calculated results are in good agreement with the test results. In addition, computing memory and computing time reductions are gained from this method compared with the FEM without SIBC.

Consequently, the proposed program can be a very use-

ful tool for designing and analyzing a multi-port microwave cavity.

Acknowledgments

This work was supported in part by Korea Research Foundation Grant (KRF2000-EA0044).

References

[1] H. Hoole, "Experimental Validation of the Impedance Boundary Condition and a Review of its Limitations," *IEEE Transactions on Magnetics*, vol. 25, no. 4, pp. 3028-3030, July 1989.

[2] F.-Z Louai, D. Benzerga, M. Feliachi, and F. Bouillault, "A 3D Finite Element Analysis Coupled to the Impedance Boundary Condition for the Magnetodynamic Problem in Radio Frequency Plasma Devices," *IEEE Transactions on Magnetics*, vol. 32, no. 3, pp. 812-815, May 1996.

[3] J. W. Shin, P. S Shin and C. Y Cheon, "Analysis of Circulator Using Hybrid Finite Element Method," *Journal of KIEE*, vol. 46, no. 5, pp. 68-73, May 1997.

[4] N. Ida and S. Yuferev, "Impedance Boundary Condition for Transient Scattering Problems," *IEEE Traansactions on Magnetics*, vol. 33, no. 2, pp. 1444-1447, March 1997.

[5] S. M. Mimoune, J. Fouladgar, A. Chentouf and G. Develey, "A 3D Impedance Calculation for an Induction Heating System for Materials with Poor Conductivity," *IEEE Transactions on Magnetics,* vol. 32, no. 3, pp. 1605-1608, May 1996.

[6] P. H. Lee, C. Y. Cheon and P. S. Shin, "Input Impedance Analysis of the Coaxial to Waveguide Type Devices," *Journal of KIEE*, vol. 34D, no. 11, pp. 9-19, November 1997.

[7] H.-B. Lee, *Computer Aided Optimal Design Methods for Waveguide Structures*, Ph.D. Dissertation, Seoul Nation University, Seoul, Korea, pp. 9-24, 1995.

[8] R. W. Freund, "Conjugate Gradient-Type Methods for Linear Systems with Complex Symmetric Coefficient matrices," *SIAM Journal of Science, Statistics, and Computation,* vol. 13. no. 1, pp. 425-448, January 1992.

Pan Seok Shin

He received the B.S. degree in Electrical Engineering from Seoul National University in 1977 and the M.S. and Ph.D. degrees in Electric Power Engineering from Rensselaer Polytechnic Institute in 1986 and 1989, respectively. From 1980-1993, he worked at the Korea Electrotechnology Research Institute as a researcher for projects involving magnetically levitated vehicles, various motors, and linear actuators. In 1993, he joined the Electrical Engineering Department of Hongik University as a professor. His teaching and research interests are analysis of electromagnetic fields, electric machinery, special actuators, and optimization techniques.

Changyul Cheon

He received the B.S. degree and the M.S. degree in Electrical Engineering from Seoul National University, Seoul, Korea in 1983 and 1985, respectively, and the Ph.D. degree in Electrical Engineering from University of Michigan at Ann Arbor in 1992. From 1992 to 1995, he was with the Department of Electrical Engineering, Kangwon National University, Chuncheon, Korea, as an assistant professor. He is currently an associate professor of Electrical Engineering at the University of Seoul, Seoul, Korea. His group at the University is currently involved with the design and analysis of microwave and millimeter-wave passive device using FEM, FDTD, and moment method techniques. He is also interested in high power microwave systems for military and commercial applications.

Sheppard J. Salon

He graduated with a B.E. degree in Engineering Science from the State University of New York at Stony Brook, an M.S. degree in Electrical Engineering from Carnegie Mellon University, and a Ph.D. degree in Electrical Engineering from the University of Pittsburgh. From 1970 to 1978 he was with the Large Rotating Apparatus Division of Westinghouse Electric Corporation in Pittsburgh, PA. He joined Rensselaer Polytechnic Institute in 1978 where he is now Professor of Electric Power Engineering. Dr. Salon is a registered professional engineer and an IEEE fellow.